Quantitative structure-activity relationships for the nucleophilicity of trivalent boron compounds

Diego García-López,[a] Jessica Cid,[a] Ruben Marqués,[a] Elena Fernández[a] and Jorge J. Carbó[a],*

Dedication ((optional))

Abstract: We describe the development of quantitative structure-activity relationships (QSAR) for the nucleophilicity of trivalent boron compounds covering boryl fragments bonded to alkali and alkali-earth metals, to transition metals, and to B(sp^3) units in diboron reagents. We used the charge of the boryl fragment (*q[B]*) and the boron p/s-population ratio (*p/s*) to describe the electronic structure of boryl moieties, whereas the *distance-weighted volume* (V_W) descriptor was used to evthe steric effects. The 3-terms easy-to-interpret QSAR model showed statistical significance and predictive ability (r^2= 0.88, q^2 = 0.83). The use of chemically meaningful descriptors identifies the factors governing the boron nucleophilicity and indicates that the most efficient nucleophiles are those that enhance the polarization of the B-X bond towards the boron atom and reduce their steric bulk. Detailed analysis of the potential energy surfaces for different type of boron substituents provides insight into the mechanism and establishes a nucleophilicity order for boron in B-X: X = Li > Cu > B(sp^3) > Pd. Finally, we use the QSAR model to make *a priori* predictions of experimentally untested compounds.

Introduction

Boryl transition-metal complexes have stimulated the synthesis of organoboron compounds since its discovery.[1] The first crystal structure analyses of boryl-metal complexes were not published until 1990, when BRR' = borabicyclo[3.3.l]nonyl was linked to iridium (III) center forming a trigonal-planar boryl ligand (sum of angles about B = 359°) and the Ir-B bond distance, 2.093(7).[2] Even in this early example it has been suggested that dπ-pπ backbonding from Ir to B to compensate the electronic deficiency on B, is weak. Therefore, boryl transition-metal complexes have largely been regarded as reagents that contain an electrophilic BRR' moiety to react with nucleophiles in a stoichiometric and catalytic way. However, the nature of the transition metal might switch the reactivity of the boryl moiety from electrophilic to nucleophilic character, and in addition the nature of the B substituents may also affect the sigma interaction between the boron and the metal, and therefore the boron's potential nucleophilicity.[3],[4] The need of a powerful method to predict the electronic behavior of boryl transition-metal complexes is fundamental for experimentalists to consider a design a la carte of the best M-BRR' reagent to guarantee a precise reactivity.

DFT methods have proven to be powerful tools to characterize the nucleophilicity of specific boryl species through the location and analysis of the corresponding transition state (TS) on the potential energy surface (PES). Thus, these kind of calculations has shown that trivalent boron compounds can react with suitable electrophilic reagents when boron is bonded to a main-group metal such as lithium,[5] to a transition metal such as copper,[6] and to a sp^3-hybridized boryl unit.[7] Alternatively, one could use more sophisticated computational methods, based on quantitative structure–activity relationship (QSAR) or –property relationship (QSPR) approaches, which are analogous to those used in drug design.[8] One of the most attractive aspects of these methods is that they generate simple equations, which allow predicting catalytic activity or selectivity a priori. Although QSAR techniques are not of common use in transition-metal chemistry, there are some outstanding examples that correlate catalytic activity and selectivity.[9],[10] It is worth to note that predicting the reactivity or designing *de novo* compounds with these approaches is quite challenging and present some limitations as recent reviews discuss in detail.[11],[12] In particular, Fey and Jover have pointed out that predictive computational chemistry can lead to promising suggestions but it is limited into the context of related compounds due to the difficulties of sampling the chemical space widely.[12]

Recently, we analyzed systematically the electronic features of several types of boryl moieties by evaluating the charge of the boryl fragment and the boron p/s-population ratio.[3] Using these easily accessible parameters of the ground-state structures, we were able to construct a qualitative tendency map, which established a gradient of nucleophilic character. As a step forward, here we seek for quantitative relationships between the structure of trivalent boron compounds and the nucleophilicity. To this end, in addition to previous electronic descriptors, we employed a steric descriptor, the *distance-weighted volume* (V_W),[13],[14] and defined a dataset of boryl units bonded to alkali and alkali-earth metals, transition metals and also bonded to B(sp^3) units in diboron reagents activated with Lewis bases. We also perform *a priori* predictions of experimentally untested compounds, evaluating externally the QSAR model.

Results and Discussion

Data set and structure generation. Figure 1 collects the trivalent boron compounds used for the QSAR modeling of boron nucleophilic activity. The library of 17 species is selected

[a] D. García-López, Dr. J. Cid, R. Marqués, Dr. E. Fernández, Dr. J. J. Carbó
Departament de Química Física i Inorgànica, Universitat Rovira i Virgili
Marcel·lí Domingo, 1, 43007 Tarragona (Spain)
E-mail: j.carbo@urv.cat

Supporting information for this article is given via a link at the end of the document.((Please delete this text if not appropriate))

from our previous bibliographic revision[4] and tendency map construction.[3] We chosen 3-4 representative structures of each boryl class, and incorporated additional rhodium and iridium complexes in order to avoid non-balanced or biased dataset (see below). Thus, the new dataset covers the full range of chemical space, including the different prototypes of nucleophilic and electrophilic boron reagents in a balanced manner. These prototypes can be divided in four categories: 1) nucleophilic reagents with boryl fragments bonded to alkali and alkali-earth metals (**1**-**4**), 2) nucleophilic diboron compounds activated by Lewis bases (**5**-**7**), 3) nucleophilic reagents with boryl fragments bonded to transition metals such as Cu and Sc (**8**-**10**), and 4) electrophilic boron reagents with the boron bonded to transition metals such as Pd, Ir and Rh (**11**-**17**). For example, the potential nucleophilic character of lithioboranes was predicted computationally.[5] And later, a diamino-substitued boryllithium compound (**2**) was isolated and reported to react with several organic electrophiles.[15] The analogous borylmagnesium compound (**4**) also reacts as a nucleophile but its reaction outcome is different.[16] In the case of benzaldehyde substrate, the boryllithium gave the α-borylbenzyl alcohol,[15] whereas the borylmagnesium afforded a mixture of products in which benzoylborane was the main product.[16] The activation of diboron compounds by Lewis bases can also generate nucleophilic boryl moieties.[4],[17],[18] The quaternisation of one boron by the base polarizes the B-B bond inducing nucleophilic character on the sp^2 boron.[7] Here, we considered adducts derived from intermolecular alkoxide activation of symmetric bis(pinacolato)diboron, $Bpin_2$, (**5**)[7],[19] and unsymmetrical diboron Bpin-Bdan (**6**);[20] as well as the intramolecular activation by N atom in the pinacolato diisopropanolaminato diboron (**7**).[21]

Moving to boryl-transition-metal complexes, we noted that their reactivity switches depending on the nature of the transition metal. One striking example is the reactivity of borylcopper and –palladium complexes with the same substrate. The borylcopper complexes behave as nucleophiles[22] and β-borate the α,β-unsaturated carbonyl ketones.[23] On the other hand, the borylpalladium *trans*-[Pd(B(NMeCH$_2$-CH$_2$-NMe))(Cl)(PMe$_2$)$_2$] complex (**11**) reacts as an electrophile providing the 1,4-additon product in which the boryl unit was bonded to the oxygen atom.[24] Thus, we selected complex **11** and gauged the electrophilic character of Pd complexes by replacing the boryl unit (**12**), and then the ligands (**13**), see Figure 1. To represent borylcopper species, we analyzed the isolated complex [Cu(Bpin)(NHC)] (NHC = 1,3-bis(2,6-diisopropyl)phenyl imidazol-2-ylidene) (**8**),[25] which also behaves as nucleophile reducing CO_2; and the analogous virtual complex [Cu(NMeCH$_2$-CH$_2$-NMe)(NHC)] (**9**), which differs in the nature of boryl ligand. Another example of transition metal supporting a nucleophilic boryl moiety is the borylscandium complex [Sc(CH$_2$SiMe$_3$)$_2$(THF)$_n$(B(NDippCH)$_2$)] (Dipp = 2,6-diisopropylphenyl) (**10**), which can undergo insertion reactions with CO yielding a product with the boron atom bonded to the carbon atom.[26] Finally, in order to balance the training dataset, we included the borylrhodium and –iridium complexes which are expected to behave as electrophiles. The rhodium structures **14** and **15** are analogous to the complex used in the first confirmed example of insertion of an alkene into the Rh-B bonds.[27] Similarly, the boryliridium complex [Ir(Me$_3$P)$_3$(Cl)(H)(Bcat)] (**16**) was synthesized and employed as catalyst in the hydroboration of alkynes.[28] Then, replacing the Bcat ligand by Bpin we obtained the complex **17**.

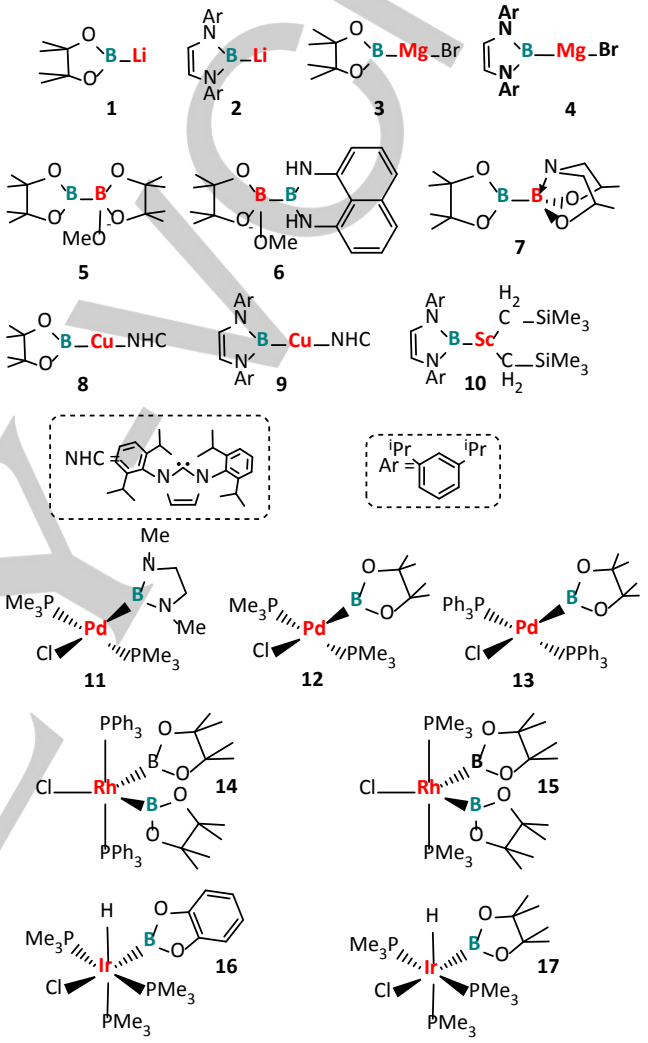

Figure 1. Selected data set of trivalent boron-containing compounds

Descriptors correlating nucleophilicity. In the multidimensional modeling, several molecular descriptors were related to the boron nucleophilicity through multivariate regression techniques. They were obtained from the ground-state structures depicted in Figure 1. Note that relying on ground-state properties for predicting the activity of novel compounds avoids the difficult, and sometimes elusive, determination of transition states and characterization of the full mechanism. In a previous contribution we identified two electronic descriptors, the overall charge of the boryl fragment (*q[B]*) and the boron p/s-population ratio (*p/s*), which were able

to classify qualitatively the nucluephilic character of boryl moieties.[3] The projection of 23 compounds onto the plot, mapping the two electronic descriptors, showed a clear clustering of the species. The clusters identified from visual analysis were closely related to the chemical nature of the atom bonded to boron and to the observed nucleophilic character.

The *q[B]* descriptor measures the charge that is supported by the overall boryl fragment computed as the sum of all the NBO atomic charges. Replacing the metal fragment in M-Bpin complexes $[Rh(Bpin)_2Cl(PMe_3)_2]$, [Cu(Bpin)(NHC)], and [Li(Bpin)], the computed activation barriers for the nucleophilic addition of Bpin to formaldehyde (50.6, 16.4 and 2.0 kcal·mol^{-1}, respectively) correlate with the overall charge of Bpin moiety (+0.13, -0.43 and -0.59 a.u., respectively). Thus, the more negatively charged the boryl fragment, the lower is the energy barrier. The *p/s* descriptor is the boron p/s-population ratio of atomic orbitals in the B-X σ-bond within NBO partition scheme. It was first introduced by Lin and Marder to gauge the polarity of boron-transition metal bonds, concluding that the greater the s character is, the more polarized the bond becomes towards the B atom.[29] We also observed that in strongly polar B-X bonds, the less s character the more-reactive the boryl fragment is as a nucleophile.[3] In the lithioboranes $(CH_3)_2BLi$, H_2BLi, and F_2BLi, computational studies by Schleyer *et al.* established the following nucleophilicity trend for boryl fragments $F_2B < H_2B < (CH_3)_2B$.[5] Here, we found that within this series, the nucleophilicity correlates with the increase of p/s ratio (1.4, 2.1 and 2.7, respectively) but not with the increase of negative charge at the boryl moiety (-0.54, -0.54 and -0.47, respectively). Therefore it is reasonable to assert that the *q[B]* provides an indication of the nucleophilic character that is induced by its counterpart, whereas the B *p/s* ratio gives a measure of the intrinsic nucleophilicity of the boryl fragment.

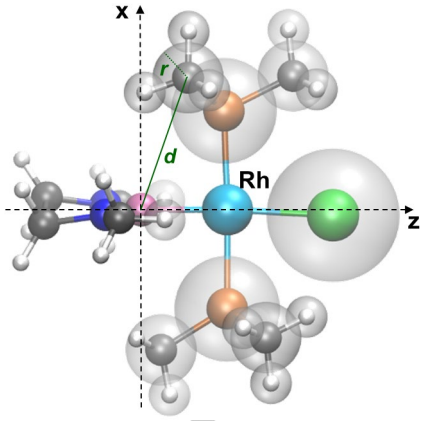

Figure 2. Illustration of the determination of the *distance-weighted volume* (V_W) descriptor for the $[Rh(Me_3P)_3Rh(Cl)(Bcat)_2]$ (**15**).

In a step forward, we introduced an additional descriptor for evaluating the steric effects of boron environment on the reactivity. We selected the *distance-weighted volume* (V_w) parameter,[13],[14] which measures the steric bulkiness of the molecular environment and its impact on the boron center. The calculation of V_w entails the alignment of boron compounds as follows: the B atom is placed at the origin with the bonded metal (X atom) along the positive z axis (see Figure 2). Then, we quantify the bulk produced by the atoms in the front side of the boron (z > 0) considering three parameters: 1) the number of atoms, excluding X, in the region defined by the alignment hypothesis, 2) the size of the atom (r = van der Waals radii), and 3) the distance (d) from the atom to the boron centre. The factor r^3 was divided by d for each atom and the sum was extended for all of the atoms in the given region (see equation 1).

$$V_W = \sum_{i=1}^{N} \frac{r_i^3}{d_i} \qquad (1)$$

Response variable and mechanistic insight. In this case there are not experimentally recorded activities that encompass broad range of trivalent boron compounds at comparable experimental conditions, precluding their simultaneous use in multivariate modeling. Therefore, the response variables measuring nucleophilicity were derived from DFT calculations. These were determined as the free-energy barriers required to transfer the boryl moiety to the electrophilic carbon atom of the model formaldehyde substrate ($\Delta G^{\neq}_{Nu}$). As Figure 3 illustrates, formaldehyde provides a simple species with an electrophilic and nucleophilic counterparts, allowing to identify and quantify the reactivity character of boron compounds.

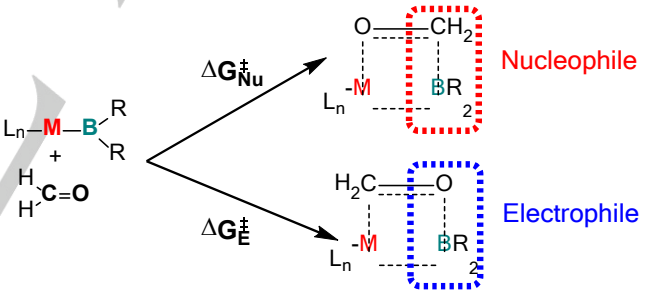

Figure 3. Evaluation of the nucleophilic and electrophilic reactivity of trivalent boron compounds using aldehyde as a model substrate.

To check the reliability of our approach and to gain additional mechanistic insight, we have analyzed in more detail the potential energy profiles for four prototypical boryl fragments bonded to Cu, Pd, Li, and B(sp^3), using formaldehyde as a model substrate. Figures 4 and 5 depict the computed free-energy profiles and Figures S1, S2, S3 and S4 show representative molecular structures and selected geometrical parameters. Marder and Lin have already used this model substrate to demonstrate that the boryl ligand in (NHC)Cu(Bpin) complex (**8**) has nucleophilic character.[6] Figure 4A shows the essential stationary points of electrophilic and nucleophilic paths. For the sake of simplicity, we omitted the two shallow η^2-aldehyde intermediates that can be formed when the substrate approaches to the copper center.[6] The boryl ligand preferentially migrates to the carbon atom leading the (NHC)Cu-

O-CH_2Bpin complex as the kinetic product. At our computational level, the free-energy barrier (16.4 kcal.mol^{-1}) is significantly lower than that for the electrophilic boryl migration to the oxygen atom of the aldehyde (40.8 kcal.mol^{-1}).

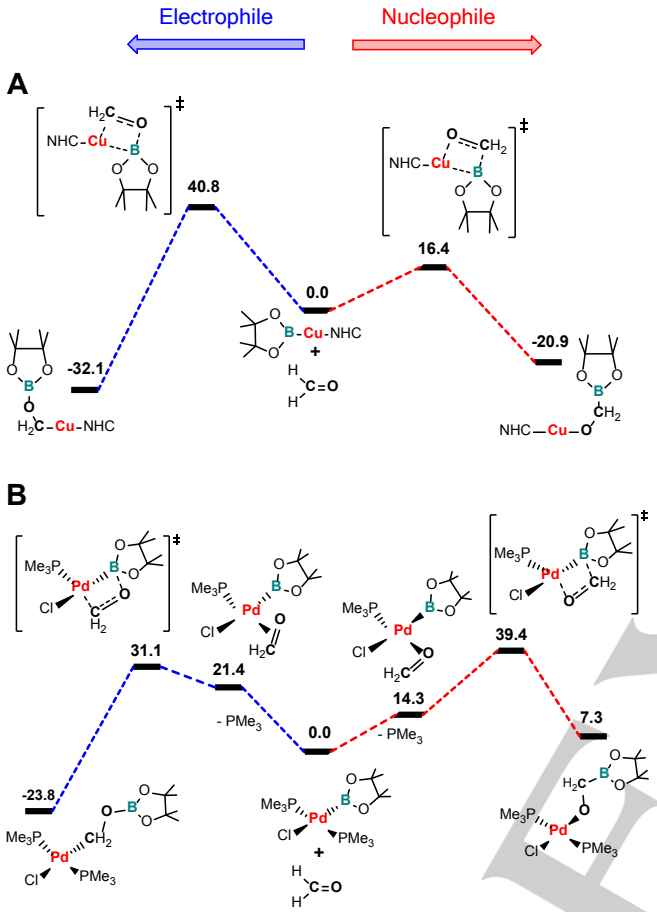

Figure 4. Free energy profiles (kcal.mol^{-1}) for the electrophilic and nucleophilic paths of aldehyde boration by the borylcopper [Cu(Bpin)(NHC)] complex (**8**) and the borylpalladium *trans*-[Pd(Bpin))(Cl)(PMe_2)$_2$] complex (**12**).

For the electrophilic borylpalladium [Pd(Bpin)Cl(PMe_3)$_2$] complex (**12**), the trend is inverted and the electrophilic path becomes kinetically favored over the nucleophilic path (Figure 4B). Previously, Wu *et al.* had characterized computationally the mechanism for Pd-catalyzed alkyne cyanoboration, where the rate determining step was found to be the insertion of the carbon-carbon triple bond into Pd-B bond.[30] The formation of the key intermediate, [Pd(BX_2)Cl(HCCH)(PH_3)], involves one phosphine dissociation and the coordination of the π-substrate. Based on these findings, we propose a dissociative mechanism involving inner sphere insertion of the substrate into the Pd-B bond (Figure 4B). Thus, complex **12** dissociates one of the PMe_3 ligands with a moderate energy cost (~20 kcal.mol^{-1}); and then, the aldehyde coordinates either via the oxygen (η^1-O) or through the carbon-oxygen π-bond, η^2-(C,O). The relative free-energies of the corresponding intermediates are high above reactants, +14.3 and +21.4 kcal.mol^{-1}, respectively. Since the electrophilic reactivity forms an alkyl palladium complex, the transition state for the insertion into the Pd-B bond should connect to the η^2-(C,O) π-complex, whereas for the nucleophilic path, the formation of the palladium-alkoxyde product could occur directly from the η^1-O σ-complex. Overall, however, the ligand/substrate exchange process occurs at lower energy than the aldehyde insertion, which is the step governing the borylpalladium activity. Thus, the calculations predict a global free-energy barrier of 31.1 kcal.mol^{-1} for electrophilic boryl migration and of 39.4 kcal.mol^{-1} for the nuclophilic one. This result is consistent with what it was observed in the boration of α,β-unsaturated carbonyl ketones by palladium complexes.[24]

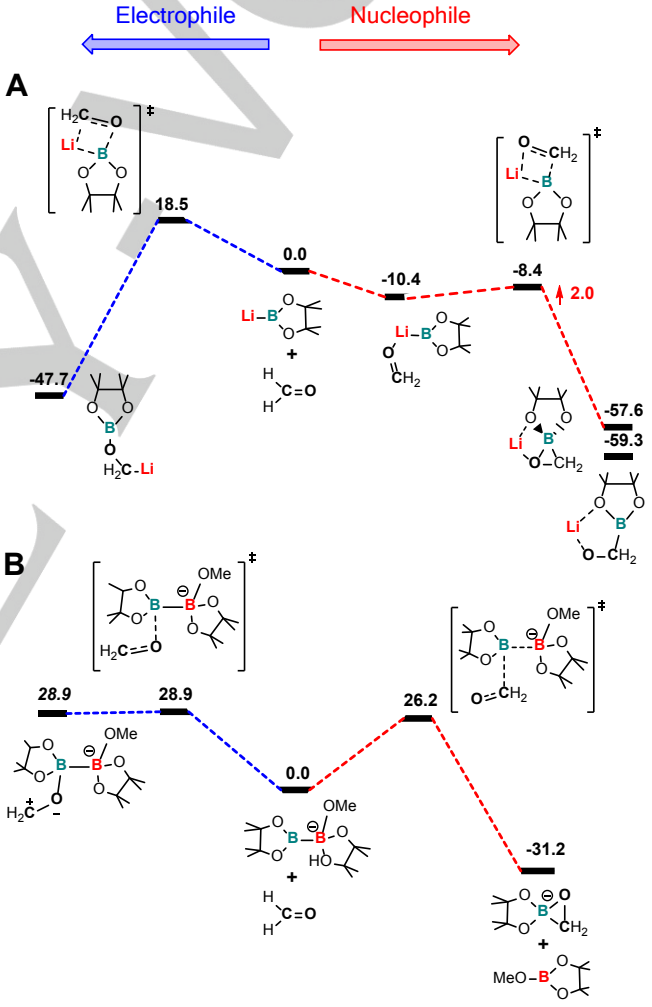

Figure 5. Free energy profiles (kcal.mol^{-1}) for the electrophilic and nucleophilic paths of aldehyde boration by the lithioborane compound [Li(Bpin)] (**1**) and the diborn compound MeO^-→Bpin-Bpin (**5**).

The nucleophilic addition of lithioboranes to formaldehyde[5] and to organohalides[31] have been already studied computationally. The former study analyzed the model lithioboranes Li$B(CH_3)_2$,

H_2BLi, and F_2BLi,[5] which initially interact with the substrate forming precursor complexes with carbonyl oxygen coordinated side-on to lithium. After overcoming low activation barriers, these precursors yield three-membered B-C-O ring product structures with a dative boron-oxygen bond.[5] In the case of the more realistic LiBpin (**1**), we obtained a similar energy profile (see Figure 5A): the free-energy of precursor formation is -10.4 kcal.mol^{-1}, the barrier is low, 2.0 kcal.mol^{-1}, and the overall process is exergonic by -57.6 kcal.mol^{-1}. Interestingly, we found another isomeric product slightly lower in energy (-59.3 kcal.mol^{-1} respect to reactants) forming a five-membered O-B-C-O-Li structure. For the novel electrophilic path, we were unable to locate a minimum with the carbonyl oxygen coordinated to boron. The aldehyde approach conducts directly to the transition state, in which a new B-O bond is formed and the lithium migrates occupying a bridging position over the oxygen-carbon bond of the substrate. The computed free-energy barrier (18.5 kcal.mol^{-1}) is significantly higher than that for the nucleophilic reaction, proving the nucleophilic character of lithioboranes.

Finally, we analyzed the reactivity of a diboron compound activated with a Lewis base, MeO^-→Bpin-Bpin (**5**), see Figure 5B. Previous DFT studies had already demonstrated the nucleophilic character of B(sp^2) moiety towards suitable electrophilic reagents,[7],[20] but its reactivity towards the nucleophilic counterparts has not been yet explored. Figure 5B shows that the nucleophilic attack of the sp^2 boron moiety at the carbonyl carbon has a free-energy barrier of 26.2 kcal.mol^{-1}, qualitatively close to that previously computed for styrene.[7] As shown previously for alkenes,[7] the transition state can rearrange to a "monoborated" anionic product with three-membered ring B-C-O structure and (pin)BOMe compound. The process develops a negative charge at the carbonyl oxygen that it is better delocalized through pinacolboryl unit, inducing the formation of the cycle. The attack of the sp^2 boron moiety at the carbonyl oxygen is different in nature. The electrophilic boron approaches in-plane to the aldehyde in order to interact with the oxygen lone pairs, whereas the nucleophilic attack of the diboron occurred perpendicular to the molecular plane to interact with the π-antibonding C=O orbital. We computed a free-energy barrier of 28.9 kcal.mol^{-1} for the addition of the carbonyl oxygen to the sp^2 boron, resulting in a high-energy shallow intermediate,[32] from which the reaction can easily proceed backwards (see Figure 5B). Additionally, we could characterize another transition state connecting the intermediate with the monoborated anionic product that is isoenergetic to the TS for backward reaction. In the additional TS, the newly quaternized boron atom becomes more negative and capable of interacting with the positively charged carbonyl carbon releasing the (pin)BOMe fragment through B-B bond cleavage (see Figure S5 for details).

The overall analysis of the four potential energy profiles demonstrates that the aldehyde substrate can serve as a model for predicting the nucleophilic / electrophilic activity of the full range of trivalent boron compounds. Within the body of examples, the relative height of computed energy barriers predict the right reactivity character observed experimentally, that is, nucleophilic character for boryl fragmentes bonded to Li, Cu and B(sp^3), and electrophilic character for borylpalladium species (see Figures 4 and 5). Moreover, we identified a nucleophilic reactivity order, Li > Cu > B(sp^2)-B(sp^3) > Pd from the computed $\Delta G^{\neq}_{Nu}$ bariers (2, 16.4, 26.2 and 39.4 kcal.mol^{-1}, respectively), which is fully consistent with experimental experience. In addition, this supports the use of nucleophilic free-energy barrier as a response variable in the QSAR modeling.

Table 1. Computed nucleophilic free-energy barriers ($\Delta G^{\neq}_{Nu}$) and values of the molecular descriptors: *p/s* atomic orbital ratio in the B-X σ-bond, charge of the boryl fragment (*q[B]*), and distance-weighted volume (V_W) employed for the trivalent boron compounds **1**-**17**.[a]

Compund	$\Delta G^{\neq}_{Nu}$	*p/s*	*q[B]*[c]	V_W
1	2.0	1.48	-0.59	0.0
2	3.6	1.51	-0.63	8.7
3	4.5	1.58	-0.42	1.3
4	8.5	1.49	-0.43	12.6
5	26.2	1.05	-0.13	17.0
6	29.1	1.15	-0.15	16.9
7	38.3	1.19	-0.02	15.1
8	16.4	0.94	-0.43	33.0
9	26.9	1.25	-0.45	46.6
10	5.5	1.03	-0.30	25.4
11	36.1	1.47	0.02	18.1
12	39.4	1.47	0.02	16.7
13	29.2	1.14	-0.02	38.4
14	58.7	1.21	0.09	47.9
15	50.6	1.39	0.13	28.2
16	44.1	1.22	0.12	25.2
17	47.2	1.52	0.17	25.8

[a] Free-energy barriers in kcal.mol^{-1} and charges of boryl fragment in a.u.

Table 1, second column, collects the $\Delta G^{\neq}_{Nu}$ values for all the selected trivalent boron compounds. The span in nucleophilicity, more than 50 kcal.mol^{-1}, indicates that the nature of the substituent has a profound influence on the reactivity character of trivalent boron. They can be roughly classified into three classes: 1) the nucleophilic boryl fragments bonded to alkali-, alkali-earth metals, scandium, and copper exhibiting free-energy barriers ranging from 2 to 27 kcal.mol^{-1} (**1**-**4**, **8**-**10**); 2) the electrophilic ones, which are bonded to late-transition metals

and have barriers ranging from 29 to 59 kcal.mol^{-1} (**11**-**17**); and 3) the ones with moderate nucleophilicity, which correspond to activated diboron compounds with free-energy barriers ranging from 26 to 38 kcal.mol^{-1} (**5**-**7**). Note that within the first group the diamino-substituted boryl copper complex (**9**) has the highest barrier, which is significantly higher than the previous one in the series. As we discuss below, this is because its crowded reaction center might lower its nuclophilicity. The ancillary ligands of transition metals can influence the reactivity in different directions. In the dissociation mechanism of borylpalladium complexes, replacing the PMe_3 ligand in **12** by the lees basic phosphine PPh_3 in **13** reduces the nucleophilec free-energy barrier in ~10 kcal.mol^{-1}, because the coordinated aldehyde becomes more electrophilic towards the boryl moiety. Conversely, for the associative mechanism of borylrhodium complexes, the same phosphine replacement (from PMe_3 in **15** to PPh_3 in **14**) increases the $\Delta G^{\neq}_{Nu}$ in ~8 kcal.mol^{-1} due to the higher bulkiness of PPh_3 in **14**.

QSAR modeling and interpretation. The calculated nucleophilicities ($\Delta G^{\neq}_{Nu}$ heights) for the representative set of complexes were correlated to the molecular descriptors (*p/s*, *q[B]* and V_w) using partial least squares regression (PLSR). Table 1 collects the computed values of the nuleophilicities and the descriptors for the different compounds. For evaluating the predicting ability of the QSAR models we employed the Pearson correlation coefficient (r^2) of the fitting stage and the predictive ability (q^2) calculated using the Leave-One-Out (LOO) cross-validation method (see Computational Details for a complete description of methodology). Table 2 shows the statistical parameters for the validation of multivariate models using different combinations of descriptors.

Initially, we built a QSAR model for predicting nucleophilicity values selecting the two electronic descriptors used for the construction of the previous tendency map,[3] the *q[B]* and the *p/s*. After the full cross-validation of the 17 compounds, r^2 of the fitting is 0.82, whereas the q^2 of the prediction is 0.78 with one PLS (first entry, Table 2). In drug design, a model is considered to be predictive when the q^2 is higher than 0.5 (halfway between perfect prediction 1.0 and no model at all 0.0). Thus, the value of 0.78 for q^2 indicates that the model can be considered predictive and that previous tendency map had a hidden quantitative relationship. Introducing the steric descriptor, V_W, the statistical parameters improve significantly (r^2 = 0.88 and q^2 = 0.83, second entry of Table 2), revealing that not only the electronic effects but the steric effects have a marked influence in determining the reactivity of these compounds. For example, the computed $\Delta G^{\neq}_{Nu}$ for **8** (16.4 kcal.mol^{-1}) is significantly lower than that of the analogous borylcopper complex **9** with a much bulkier boryl fragment (26.9 kcal.mol^{-1}). In fact, the QSAR model with the two electronic parameters predicts the wrong nucleophilicity order for these complexes (12.3 and 10.9 kcal.mol^{-1} for **8** and **9** in the fitting stage), whereas the QSAR model with the steric parameter predicts the right order and values that are closer to the response variables (17.1 and 19.9 kcal.mol^{-1} for **8** and **9** in the fitting stage).

$$\Delta G^{\neq}_{Nu} = a_0 + \sum_{i=1}^{3} a_i D_i + \sum_{i=1}^{3} b_i D_i^2 + \sum_{i=1}^{3} \sum_{j>1}^{3} c_{ij} D_i D_j \qquad (2)$$

To try to improve data description, we fitted the nucleophilicities to polynomial functions including higher-order and crossing terms. As represented by equation (2), we built polynomials which include the descriptors raised to the second power, D_i^2, in order to account for the possible deviations of linearity in the correlation, and the D_iD_j crossing terms evaluating the possible interplay between descriptors. When the higher-order, the crossing, or all the possible terms of the equation were considered, the new models did not improve appreciably the correlation of the data nor the predicting ability (r^2 = 0.87, 0.90 and 0.90 and q^2 = 0.83, 0.83 and 0.82, respectively; see Table 2). This indicates that there is a linear relationship between $\Delta G^{\neq}_{Nu}$ and the defined descriptors, and that these descriptors are independent to each other and describes different chemical features. Thus, for further analyses, we selected the simpler QSAR model fitted to first-order polynomials with three variables.

Table 2. Statistical parameters of the leave-one-out cross-validation for $\Delta G^{\neq}_{Nu}$ by using different descriptors.[a]

Descriptor	r^2	q^2
p/s, *q[B]*	0.82	0.78
p/s, *q[B]*, V_W	0.88	0.83
p/s, *q[B]*, V_W, $(p/s)^2$, $(q[B])^2$, $(V_W)^2$	0.87	0.83
p/s, *q[B]*, V_W, (*p/s* • *q[B]*), (*p/s* • V_W), (*q[B]* • V_W)	0.90	0.83
all	0.90	0.82

[a] Slope (fitting/prediction), intercept (fitting/predition) in kcal•mol^{-1} and error (fitting/prediction) in kcal•mol^{-1}: 0.83/0.80, 4.8/5.4 and 7.1/8.3 for model in entry 1; 0.88/0.85, 3.4/4.1 and 6.2/7.1 for model in entry 2; 0.87/0.84, 3.6/4.3 and 6.3/7.2 for model in entry 3; 0.90/0.87, 2.9/3.3 and 5.7/7.3 for model in entry 4; 0.90/0.86, 2.8/3.3 and 5.6/7.6 for model in entry 5.

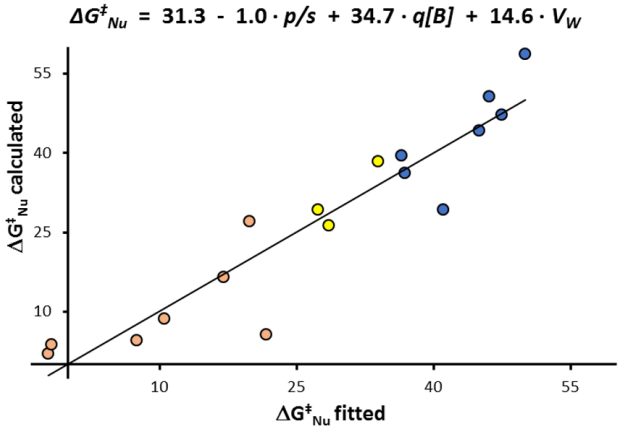

Figure 6. Calculated versus fitted free-energy barriers in kcal.mol^{-1} for the dataset of 17 compounds using the first-order polynomial with *p/s*, *q[B]* and V_W descriptors; and the resulting QSAR equation. Circles in red correspond to strong nuclophiles, in yellow to moderate nucleophiles, and in blue to electrophiles.

Figure 6 shows the computed $\Delta G^{\neq}_{Nu}$ values plotted against the fitted $\Delta G^{\neq}_{Nu}$ values and the coefficients of QSAR equation for the first-order polynomial with three variable (see also Eq. S1 in Supporting Information). The graph uses a color code to distinguish between the different classes of compounds defined above: the strong nucleophilic (red circles), the electrophilic (blue circles) and those with a moderate nucleophilic character (yellow circles). The correlation is fairly good for all compounds, the largest residual being observed for compound **10**, borylscandium (Figure S5). A more accurate inspection shows that this is the only early transition-metal complex in the dataset explaining the difficulties to predict it. QSAR methods require a wide sampling of the chemical space, which is not available here for early transition-metals, in order to produce accurate predictions.[12]

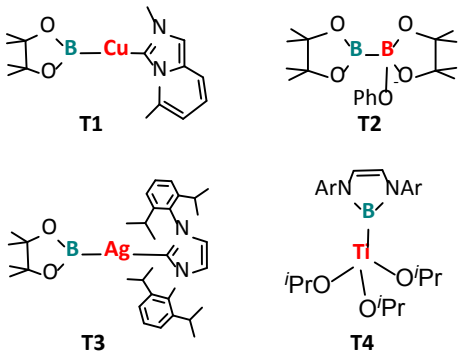

Figure 7. Selected trivalent boron compounds for the external blind test.

Table 3. Calculated versus predicted free-energy barriers ($\Delta G^{\neq}_{Nu}$ in kcal.mol^{-1}) for a blind test subset (N = 4) employing the three-parameters QSAR model generated from the initial set (N = 17).

Label	Compound	$\Delta G^{\neq}_{Nu}$ calc.	$\Delta G^{\neq}_{Nu}$ predicted
T1	[Cu(Bpin)(NHC1)] [a]	14.6	13.3
T2	PhO$^-$→Bpin-Bpin	32.2	32.7
T3	[Ag(Bpin)(NHC)]	29.2	21.3
T4	[Ti(B(NAr(CH$_2$)$_2$NAr)(O^{i}Pr)$_3$]	29.2	37.9

[a] NHC1 = imidazopyridine-2-ylidene derivative

In addition to the predictive ability of the mathematical model, it is also possible to obtain additional chemical information from the analysis of the QSAR equation coefficients. Thus, the positive coefficient for the steric descriptor, V_W, indicates that reducing the steric bulk would lower the free-energy barrier and, consequently, increase the nuclophilicity of the boryl fragment. For example, the borylmagnesium compound **3** (V_W = 1.3) and the borylrhodium complex **15** (V_W = 28.2) have lower $\Delta G^{\neq}_{Nu}$ values (4.5 and 50.6 kcal.mol^{-1}, respectively) than the analogous compounds **4** and **14** (8.5 and 58.7 kcal.mol^{-1}, respectively) with bulkier boryl fragment (V_W = 12.7) and auxiliary ligands (V_W = 47.9), respectively (see Table 1 and Figure 1). The QSAR coefficient for the electrostatic *q[B]* descriptor is also positive confirming initial intuitive interpretation: the more negatively charged the boryl fragment, the lower is the energy barrier and the higher the nucleophilicity. Extending the example of previous section, the computed $\Delta G^{\neq}_{Nu}$ for compounds **15**, **12**, **5**, **8** and **1** are 50.6, 39.4, 26.2, 16.4 and 2.0 kcal·mol^{-1}, respectively, while the overall charges of the Bpin moieties are +0.13, +0.02, -0.13, -0.43 and -0.59 a.u., respectively.

Finally, we noted that the value of the coefficient for the *p/s* descriptor has significantly lower weight (lower absolute value) compared to the other two descriptors, indicating that *p/s* ratio has not a big influence in determining nucleophilicity but it could tune it. In fact as shown above, the energy barrier on going from lithioborane $(CH_3)_2BLi$ to F_2BLi varies only in 1.3 kcal.mol^{-1} despite of the significantly chemical differences.[5] This indicates that the nature of boryl fragment is significantly less important than the nature of the bonded metal in determining the reactivity character. And consequently, it is possible to build a simpler two-term equation with *q[B]* and V_W descriptors showing very similar statistical parameters (see Figure S7). Nevertheless, we think that it is conceptually more interesting to use also the *p/s* descriptor in order to fine tune the QSAR model as a function of boryl nature.

To externally validate the QSAR model within a blind test, we tried to carry out *a priori* prediction of the performance of the 4 compounds depicted in Figure 7. Additionally, this will serve to evaluate the robustness of the model because none of the compounds were used to build or to select the parameters of the QSAR equation. We selected one ligand-modified borylcopper complex **T1**, one base-modified diboron compound **T2**, and two complexes with new metal fragments, the borylsilver **T3** and boryltitanium **T4**. Table 3 shows the calculated and the predicted $\Delta G^{\neq}_{Nu}$. We observed an excellent prediction for the two former complexes (**T1** and **T2**), whereas for the other two complexes (**T3** and **T4**), whose metal fragments bonded to boron were not in the training set, the predictions are poorer.

In **T1**, we replaced the imidazol-2-ylidene (NHC) ligand of **8** by the imidazopyridine-2-ylidene derivative (NHC1).[33] This type of carbene substitution have had a marked influence on the reactivity of gold chemistry.[34] Here, the predicted nucleophilicity for the virtual borylcopper complex **T1** is higher than for complex **8** (see Tables 1 and 3), because the steric parameter estimates a less crowded reaction center for **T1** (V_W = 33.0 and 11.8 for **8** and **T1**, respectively). Marder *et al.* have isolated a sp^2-sp^3 diborane prepared *via* the addition of aryloxide, but they did not report its reactivity.[18] Therefore, we evaluated the ability of PhO$^-$→Bpin-Bpin (**T2**) to act as source of nucleophilic boryl anions, and it turned out to be less efficient than methoxy adduct **5** ($\Delta G^{\neq}_{Nu}$ = 32.2 *vs.* 26.2 kcal.mol^{-1}). However, compound **T2** can be still classified as a moderate nucleophily.

The borylsilver complex **T3** is another virtual structure, which results from the metal replacement in the borylcopper **8**. Previous theoretical calculations on [M(Bpin)(NHC)] (M = Cu and Ag) showed that the polarity of the M-B bond increases in the order Ag^I < Cu^I; and hence, it is presumable that borylsilver species have lower nucleophilic character than borylcooper. [3]

Indeed, here we show that the $\Delta G^{\neq}_{Nu}$ values for **T3** (21.3 for prediction and 29.2 kcal.mol^{-1} for DFT calculation) are larger than that computed for **8** (16.4 kcal.mol^{-1}). Even so, the value of the barrier is within the energy range defined for moderate nucleophiles, indicating that this borylsilver complex could behave as nucleophile under certain conditions. The boryltitatinum triisopropoxide **T4** had been synthesized,[35] and its boron nucleophilic reactivity suggested.[36] Since then, however, the use of **T4** in the borylation of organic substrates has not been reported, presumably because its boryl moiety has a low reactivity. Here, the predicted $\Delta G^{\neq}_{Nu}$ value differs quantitatively from the computed one (37.9 *vs.* 29.2 kcal.mol^{-1}), but both values are within the energy range defined for moderate nucleophiles. Summarizing the external validation results, our QSAR model can predict with good precision the nucleophilic character of boryl fragments bonded to the atoms used to build QSAR equation, whereas for other metals the model seems to be limited to screening purposes. This trend is not surprising because the predicting ability of QSAR models relies on the availability of large data that samples chemical space widely.[12] With these features in hand, we propose a novel borylcopper complex as a source of strong nucleophilic boryl moieties, and that the diboranes activated with aryloxides, the borysilver and the boryltitanium complexes can show moderate to low nucleophilicity.

We also tested whether it had been possible to anticipate the nucleophilic behavior of two experimentally tested boryl compounds coming from two independent laboratories. We selected the borylzinc complex $[ZnBr_2(THF)_n(B(NDipCH)_2)]Li$ (Dip = 2,6-diisopropylphenyl),[36] **T5**; and the activated diboron $F^-\rightarrow$Bpin-Bpin, **T6**.[18]b The QSAR model predicted free-energy barriers of 15.0 and 27.7 kcal.mol^{-1}, respectively, which are in full agreement with experimental observations. The borylzinc complex **T5** was correctly classified as a *nucleophile* because its predicted $\Delta G^{\neq}_{Nu}$ (15 kcal.mol^{-1}) is into the range of the calculated values for nuclophilic boryl fragments (2 – 27 kcal.mol^{-1}, see above). Similarly, **T6** was correctly classified as a *moderate nucleophile*, its predicted $\Delta G^{\neq}_{Nu}$ value (27.7 kcal.mol^{-1}) being into the range of other activated diboron compounds acting as nucleophiles (26 – 38 kcal.mol^{-1}, see above). Thus, this external blind test demonstrates that the QSAR model is able to carry out *a priori* predictions for both **T5** and **T6** compounds further proving its predictive ability.

Conclusions

A QSAR model was generated for predicting the nucleophilicity of trivalent boron compounds using a varied dataset, which includes boryl moieties bonded to alkali- and alkali-earth-metals, coordinated to transition metals, and bonded to sp^3-hybridized boryl units. The optimal predictive model (r^2 = 0.88 , q^2 = 0.83) was obtained using the computed free-energy barrier, $\Delta G^{\neq}_{Nu}$, as a response variable and three molecular descriptors: the p/s-population ratio (*p/s*), the charge of the boryl fragment (*q[B]*) and the steric bulk evaluated with the *distance-weighted volume* (V_W) parameter. This yields a 3-terms easy-to-interpret QSAR equation that shows good predictive abilities establishing a direct connection between nucleophilicity and the properties of bonded metal fragments.

The use of chemically meaningful descriptors provides insight into the factors governing the nucleophilicity. Thus, the metal fragments that most effectively promote nucleophilic activity are those that polarize the B-M bond yielding negatively charged boryl moieties. The predictive ability of the QSAR model improved when introducing the *distance-weighted volume* to account for the steric effects induced by the metal fragments and the bulky substituents of boron. Reducing the steric bulk on the reaction center would favor substrate coordination and reactivity. In addition, the analysis of the potential energy profiles for four prototypical boryl fragments bonded to Li, B(sp^3), Cu and Pd gives detailed molecular insight into the reaction mechanisms and it establishes a nucleophilicity order: Li > Cu > B(sp^2)-B(sp^3) > Pd.

This computational methodology has been also used to make *a priori* predictions of experimentally untested compounds, evaluating externally the QSAR model. The predictions have good precision for boryl fragments bonded to any of the metals used to build the QSAR equation, whereas the model has screening ability when the nature of the metal bonded to it is outside the training dataset. We propose that borylcopper complexes with less sterically hindered N-heterocyclic carbenes could enhance their nucleophilicity. Moreover, diboranes activated with aryloxides, borysilver and boryltitanium complexes could behave as moderate nucleophiles under certain conditions. Finally, we hope this model can be straightforwardly used for *a priori* evaluation of the nucleophilic character of other trivalent boron compounds, and for deriving guidelines for novel agents design.

Experimental Section

Computational Details

Full quantum mechanical calculations were performed using the Gaussian09 series of programs.[38] Calculations were performed within the framework of DFT[39] using the B3LYP functional.[40] The basis set for transition-metals, Si, P, Cl and Br atoms was that associated with a pseudopotential with a standard double-ξ LANL2DZ contraction,[41] and the basis set was supplemented by *f* and *d* shells, respectively.[42] The rest of atoms were described with a standard 6-31G(d,p) basis set.[43] All geometry optimizations were full, with no restrictions. The nature of the minima stationary points encountered was characterized by means of harmonic vibrational frequencies analysis. The bonding situation of the molecules as well as the fragment charges, has been analysed using the NBO method,[44] from which we derived the *p/s* and *q[B]* descriptors

We used partial least-squares (PLS) regression[45] as multivariate regression technique. External and full cross-validations were considered for model building and evaluation. Different statistical parameters were employed for evaluating the predictive ability of the models during the fitting and test stages, namely, the Pearson correlation coefficient (r^2), the

determination coefficient (q^2), the sample standard error and the slope and intercept of the fitted/predicted versus observed values.[46] Since the numerical values of the descriptors can vary significantly, each set of descriptors is normalized respect to the maximum absolute value of the set in order to ensure they have equal weight in multivariate analysis.

Acknowledgements

We acknowledge support from the Spanish Ministry of Science and Innovation (grant CTQ2014-52774-P) and the Generalitat de Catalunya (2014SGR199 and XRQTC).

Keywords: Boron • nucleophilicity • DFT • QSAR • catalysis

References

[1] a) G. Schmid, H. Nöth, *Angew. Chem., Inr. Ed. Engl.* **1963**, *2*, 623; b) H. Braunschweig, *Angew. Chem. Int. Ed.* **1998**, *37*, 1786; G. J. Irvine, M. J. G. Lesley, T. B. Marder, N. C. Norman, C. R. Rice, E. G. Robins, W. R. Roper, G. R. Whittell, L. J. Wright, *Chem. Rev.* **1998**, *98*, 2685; c) S. Westcott, E. Fernández, *Adv. Organomet. Chem.,* **2015**, *63*, 39.

[2] R. T. Baker, D. W. Ovenall, J. C. Calabrese, S. A. Westcott, N. J. Taylor, I. D. Williams, T. B. Marder, *J. Am. Chem. Soc.* **1990**, *112*, 9399.

[3] J. Cid, J. J. Carbó, E. Fernández, *Chem. Eur. J.* **2012**, *18*, 12794.

[4] a) J. Cid, H. Gulyás, J. J. Carbó, E. Fernández, *Chem. Soc. Rev.*, **2012**, *41*, 3558; b) L. Dang, Z. Lin, T. B. Marder, *Chem. Commun*. **2009**, 3987

[5] M. Wagner, N.J. R. van Eikema Hommes, H. Nöth, P. v R. Schleyer *Inorg. Chem*. **1995**, *34*, 607.

[6] H. Zhao, L. Dang, T. B. Marder, Z. Lin, *J. Am. Chem. Soc.* **2008**, *130*, 5586.

[7] a) A. Bonet, C. Pubill-Ulldemolins, C. Bo, H. Gulyás, E. Fernández, *Angew. Chem. Int. Ed.* **2011**, *50*, 7158; b) C. Pubill-Ulldemolins, A. Bonet, C. Bo, H. Gulyás, E. Fernández, *Chem. Eur. J.* **2012**, *18*, 112.

[8] a) A. G. Maldonado, J. A. Hageman, S. Mastroianni, G. Rothenberg *Adv. Synth. Catal.* **2009**, *351*, 387; b) N. Fey, J. N. Harvey, *Coord. Chem. Rev.* **2009**, *253*, 704-722; c) N. Fey *Dalton Trans.* **2010**, *39*, 296; d) C. R. Corbeil, N. Moitessier, *J. Mol. Catal. A: Chem.* **2010**, *324*, 146.

[9] (a) V. L. Cruz, J. Ramos, S. Martínez, A. Muñoz-Escalona, J. Martínez-Salazar, *Organometallics*, **2005**, *24*, 5095; (b) V. L. Cruz, J. Martínez, J. Martínez-Salazar, J. Ramos, M. L. Reyes, A. Toro-Labbe, S. Gutierrez-Oliva, *Polymer*, **2007**, *48*, 7672; (c) G. Occhipinti, H. R. Bjørsvik, V. R. Jensen, *J. Am. Chem. Soc.* **2006**, *128*, 6952; (d) J. A. Hageman, J. A. Westerhuis, H. W. Frühauf, G. Rothenberg, *Adv. Synth. Catal.* **2006**, *348*, 361; (e) Z. Strassberger, M. Mooijman, E. Ruijter, A. H. Alberts, A. G. Maldonado, R. V. A. Orru, G. Rothenberg, *Adv. Synth. Catal.* **2010**, *352*, 2201; (f) T. A. Manz, J. M. Caruthers, S. Sharma, K. Phomphrai, K. T. Thomson, W. N. Delgass, M. M. Abu-Omar, *Organometallics*, **2012**, *31*,602; (g) S. Aguado-Ullate, J. A. Baker, V. González-González, C. Müller, J. D. Hirst, J. J. Carbó, *Catal. Sci. Technol.*, **2014**, *4*, 979; (h) T. A. Manz *RSC Adv.*, **2015**, *5*, 48246.

[10] (a) K. B. Lipkowitz, M. Pradhan, *J. Org. Chem.*, **2003**, *68*, 4648; (b) M. C. Kozlowski, S. Dixon, M. Panda, G. Lauri, *J. Am. Chem. Soc.*, **2003**, *125*, 6614; (c) S. Sciabola, A. Alex, P. D. Higginson, J. C. Mitchell, M. J. Snowden, I. Morao, *J. Org. Chem.*, **2005**, *70*, 9025; (d) J. C. Ianni, V. Annamalai, P.-W. Phuan, M. C. Kozlowski, *Angew. Chem., Int. Ed.*, **2006**, *45*, 5502; (e) M. Urbano-Cuadrado, J. J. Carbó, A. G. Maldonado, C. Bo, *J. Chem. Inf. Model.*, **2007**, *47*, 2228; (f) M. C. Kozlowski, J. C. Ianni, *J. Mol. Catal. A: Chem.*, **2010**, *324*, 141; (g) S. Aguado-Ullate, L. Guasch, M. Urbano-Cuadrado, C. Bo, J. J. Carbó, *Catal. Sci. Technol.*, **2012**, *2*, 1694; (h) H. Huang, H. Zong, B Shen, H. Yue, G. Bian, L. Song, *Tetrahedron*, **2014**, *70,* 1289.

[11] D. J. Tantillo, *Acc. Chem. Res.* **2016**, *49*, 1079; special issue on "*Computational Catalysis for Organic Synthesis*".

[12] a) N. Fey, *Chem. Central J.*, **2015**, *9*, 38; b) J. Jover, N. Fey, *Chem. Asian J.*, **2014**, *9*, 1714.

[13] a) S. Aguado-Ullate, S. Saureu, L. Guasch and J. J. Carbó, *Chem. Eur. J.*, **2012**, *18*, 995; b) S. Aguado-Ullate, M. Urbano, I. Villaba, E. Pires, J. I. García, C. Bo, J. J. Carbó, *Chem. Eur. J.*, **2012**, *18*, 14026.

[14] MolQuO application: http://rodi.urv.es/~carbo/quadrants/index.html accessed November 2016.

[15] a) Y. Segawa, M. Yamashita, K. Nozaki, *Science* **2006**, *314*, 113; b) Y. Segawa, Y. Suzuki, M. Yamashita, K. Nozaki, *J. Am. Chem. Soc.* **2008**, *130*, 16069; c) T. B. Marder, *Science*, **2006**, *314*, 64; d) . Segawa, M. Yamashita, K. Nozaki, Angew. Chem. Int. Ed. **2007**, *46*, 6710; e) M. Yamashita, K. Nozaki, *Pure Appl. Chem.* **2008**, *80*, 1187.

[16] M. Yamashita, Y. Suzuki, Y. Segawa, K. Nozaki, *J. Am. Chem. Soc.* **2007**, *129*, 9570.

[17] a) E. C. Neeve, S. J. Geier, I. A. I. Mkhalid, S. A. Westcott, T B. Marder, *Chem. Rev.*, **2016**, *116*, 9091; b) A. B. Cuenca, R. Shishido, H. Ito, E. Fernández, *Chem. Soc. Rev.*, **2016**, in press

[18] a) R. D. Dewhurst, E. C. Neeve, H. Braunschweig, T. B. Marder, *Chem. Commun.*, **2015**, *51*, 9594; b) S. Pietsch, E. C. Neeve, D. C. Apperley, R. Bertermann, F. Mo, D. Qiu, M. S. Cheung, L. Dang, J. Wang, U. Radius, Z. Lin, C. Kleeberg, T. B. Marder, *Chem. Eur. J.*, **2015**, *21*, 7082; and references therein.

[19] a) C. Solé, H. Gulyás, E. Fernández, *Chem. Comun.*, **2012**, *48*, 3769; b) C. Pubil-Ulldemolins, A. Bonet, H. Gulyás, C. Bo, E. Fernández, *Org. Biomol. Chem.*, **2012**, *10*, 9677; c) X. Sanz, G. M. Lee, C. Pubill-Ulldemolins, A. Bonet, H. Gulyás, S. A. Westcott, C. Bo, E. Fernández, *Org. Biomol. Chem.*, **2013**, *11*, 7004.

[20] a) J. Cid, J. J. Carbó, E. Fernández, *Chem. Eur. J.*, **2014**, *20*, 3616; c) N. Miralles, J. Cid, A. B. Cuenca, J. J. Carbó, E. Fernández, *Chem. Commun.,* **2015**, *51*, 1693.

[21] a) M. Gao, S. B. Thorpe, W. L. Santos, *Org. Lett.* **2009**, *11*, 3478; b) S. B. Thorpe, X. Guo, W. L. Santos, *Chem. Commun.* **2011**, *47*, 424; c) M. Gao, S. B. Thorpe, Ch. Kleeberg, C. Slebodnick, T. B. Marder, W. L. Santos, *J. Org. Chem.* **2011**, *76*, 3997.

[22] L. Dang, Z. Lin and T. B. Marder, *Organometallics*, **2008**, *27*,4443.

[23] a) H. Ito, H. Yamanaka, J. Tateiwa, A. Hosomi, *Tetrahedron Letters*, **2000**, *41*, 682; b) K. Takahashi, T. Isiyama, N. Miyaura, *Chem. Lett.*, **2000**, 982; c) K. Takahashi, T. Isiyama, N. Miyaura, *J. Organomet. Chem.*, **2001**, *625*, 47.

[24] S. Onozawa, M. Tanaka, *Organometallics*, **2001**, *20*, 2956.

[25] D. S. Laitar, P. Müller, J. P. Sadighi, *J. Am. Chem. Soc.*, **2005**, *127*, 17196.

[26] S. Li, J. Cheng, Y. Chen, M. Nishiura and Z. Hou, *Angew. Chem.*, *Int. Ed.*, **2011**, *50*, 6360.

[27] R. T. Baker, J. C. Calabrese, S. A. Westcott, P. Nguyen, T. Marder, *J. Am. Chem. Soc.*, **1993**, *115*, 4367.

[28] J. S. Merola, J. R. Knorr, *J. Organomet. Chem.*, **2014**, *750*, 86.

[29] J. Zhu, A. Lin, T. B. Marder, *Inorg. Chem.* **2005**, *44*, 9384.

[30] M. Y. Wang, L. Cheng, Z. J. Wu, *J. Comp. Chem.* **2008**, *29*, 1825.

[31] M. S. Cheung, T. B. Marder, Z. Lin, *Organometallics*, **2011**, *30*, 3018.

[32] The stationary point corresponding to the intermediate was located in the potential electronic energy surface, in which its energy was 0.02 kcal.mol^{-1} lower than the preceding transition state. However, upon addition of thermal and entropic corrections to get the Gibbs free-energies, the energy of the intermediate becomes slightly higher than the transition state (0.4 kcal.mol^{-1}) due to the approximations performed in the statistical mechanics treatment.

[33] M. Alcarazo, S. J. Roseblade, A. R. Cowley, R. Fernández, J. M. Brown, J. M. Lassaletta, *J. Am. Chem. Soc.* **2005**, *127*, 3290.

[34] M. Alcarazo, T. Stork, A. Anoop, W. Thiel, A. Fürstner, *Angew. Chem. Int. Ed.* **2010**, *49*, 2542.

[35] T. Terabayashi, T. Kajiwara, M. Yamashita, K. Nozaki, *J. Am. Chem. Soc.*, **2009**, *131*, 14162.

[36] A. V. Protchenko, L. M. A. Saleh, D. Vidovic, D. Dange, C. Jones, P. Mountford, S. Aldridge, *Chem. Commun*. **2010**, *46*, 8546.

[37] T. Kajiwara, T. Terabayashi, M. Yamashita, K. Nozaki, *Angew. Chem. Int. Ed.* **2008**, *47*, 6606.

[38] M. J. Frisch, G. W. Trucks, H. B. Schlegel, G. E. Scuseria, M. A. Robb, J. R. Cheeseman, G. Scalmani, V. Barone, B. Mennucci, G. A. Petersson, H. Nakatsuji, M. Caricato, X. Li, H. P. Hratchian, A. F. Izmaylov, J. Bloino, G. Zheng, J. L. Sonnenberg, M. Hada, M. Ehara, K. Toyota, R. Fukuda, J. Hasegawa, M. Ishida, T. Nakajima, Y. Honda, O. Kitao, H. Nakai, T. Vreven, J. A., Jr., Montgomery, J. E. Peralta, F. Ogliaro, M. Bearpark, J. J. Heyd, E. Brothers, K. N. Kudin, V. N. Staroverov, R. Kobayashi, J. Normand, K. Raghavachari, A. Rendell, J. C. Burant, S. S. Iyengar, J. Tomasi, M. Cossi, N. Rega, J. M. Millam, M. Klene, J. E. Knox, J. B. Cross, V. Bakken, C. Adamo, J. Jaramillo, R. Gomperts, R. E. Stratmann, O. Yazyev, A. J. Austin, R. Cammi, C. Pomelli, J.W. Ochterski, R. L. Martin, K. Morokuma, V. G. Zakrzewski, G. A. Voth, P. Salvador, J. J. Dannenberg, S. Dapprich, A. D. Daniels, O. Farkas, J. B. Foresman, J. V. Ortiz, J. Cioslowski, D. J. Fox, Gaussian 09, Revision A.02; Gaussian, Inc.: Wallingford, CT, **2009**.

[39] R. G. Parr, W. Yang, in *Density Functional Theory of Atoms and Molecule*, Oxford University Press, Oxford, UK, **1989**.

[40] a) C. Lee, W. Yang, R. G. Parr, *Phys. Rev. B* **1988**, *37*, 785; b) A. D. Becke, *J. Chem. Phys.* **1993**, *98*, 5648; c) P. J. Stephens, F. J. Devlin, C. F. Chabalowski, M. J. Frisch, *J. Phys. Chem.* **1994**, *98* , 11623.

[41] P. J. Hay, W. R. Wadt, J. Chem. Phys. **1985**, *82*, 299.

[42] a) A. Höllwarth, M. Böhme, S. Dapprich, A.W. Ehlers, A. Gobbi, V. Jonas, K. F. Köhler, R. Stegmann, A. Veldkamp, G. Frenking, *Chem. Phys. Lett.* **1993**, *208*, 237. b) A.W. Ehlers, M. Böhme, S. Dapprich, A. Gobbi, A. Höllwarth, V. Jonas, K.F. Köhler, R. Stegmann, A. Veldkamp, G. Frenking, *Chem. Phys. Lett.* **1993**, *208*, 111.

[43] a) M .M. Francl, W. J. Pietro, W. J. Hehre, J. S. Binkley, M. S. Gordon, D. J. Defrees, J. A. Pople, *J. Chem. Phys.* **1982**, *77*, 3654. (b) W. J. Hehre, R. Ditchfield, J. A. Pople, *J. Chem. Phys.* **1972**, *56*, 2257. (c) P. C. Hariharan, J. A. Pople, *Theor. Chim. Acta* **1973**, *28*, 213.

[44] A. E. Reed, L. A. Curtiss, F. Weinhold, *Chem. Rev.* **1985** , *88*, 899.

[45] a) S. Wold, M. Sjostrom, L. Eriksson, *Chemom. Intell. Lab. Syst.* **2001**, *58*, 109; b) P. Geladi, B. Kowalski, *Anal. Chim. Acta* **1986**, *185*,1.

[46] D. M. Hawkins, S. C. Basak, D. Mills, *J. Chem. Inf. Comput. Sci.* **2003**, *43*, 579.

FULL PAPER

We developed a QSAR model for the nucleophilicity of trivalent boron compounds that showed statistical significance and predictive ability, and allowed performing *a priori* predictions of experimentally untested compounds. The chemical space covers boryl fragments bonded to alkali and alkali-earth metals, to transition metals, and to B(sp3) units in diboron reagents activated by Lewis bases.

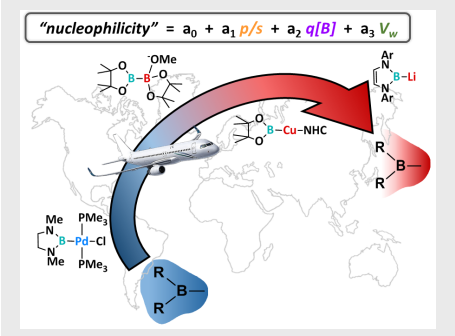

*D. García-López, J. Cid, R. Marqués, E. Fernández, J. J. Carbó**

Page No. – Page No.

Quantitative structure-activity relationships for the nucleophilicity of trivalent boron compounds